

NANO REVIEW

Open Access

Research progress on electronic phase separation in low-dimensional perovskite manganite nanostructures

Lizhi Liang, Lei Li, Heng Wu and Xinhua Zhu*

Abstract

Perovskite oxide manganites with a general formula of $R_{1-x}AxMnO_3$ (where R is a trivalent rare-earth element such as La, Pr, Sm, and A is a divalent alkaline-earth element such as Ca, Sr, and Ba) have received much attention due to their unusual electron-transport and magnetic properties, which are indispensable for applications in microelectronic, magnetic, and spintronic devices. Recent advances in the science and technology have resulted in the feature sizes of microelectronic devices based on perovskite manganite oxides down-scaling into nanoscale dimensions. At the nanoscale, low-dimensional perovskite manganite oxide nanostructures display novel physical properties that are different from their bulk and film counterparts. Recently, there is strong experimental evidence to indicate that the low-dimensional perovskite manganite oxide nanostructures are electronically inhomogeneous, consisting of different spatial regions with different electronic orders, a phenomenon that is named as electronic phase separation (EPS). As the geometry sizes of the low-dimensional manganite nanostructures are reduced to the characteristic EPS length scale (typically several tens of nanometers in manganites), the EPS is expected to be strongly modulated, leading to quite dramatic changes in functionality and more emergent phenomena. Therefore, reduced dimensionality opens a door to the new functionalities in perovskite manganite oxides and offers a way to gain new insight into the nature of EPS. During the past few years, much progress has been made in understanding the physical nature of the EPS in low-dimensional perovskite manganite nanostructures both from experimentalists and theorists, which have a profound impact on the oxide nanoelectronics. This nanoreview covers the research progresses of the EPS in low-dimensional perovskite manganite nanostructures such as nanoparticles, nanowires/nanotubes, and nanostructured films and/or patterns. The possible physical origins of the EPS are also discussed from the signatures of electronic inhomogeneities as well as some theoretical scenarios, to shed light on understanding this phenomenon. Finally, the perspectives to the future researches in this area are also outlined.

Keywords: Perovskite manganites; Low-dimensional nanostructures; Electronic phase separation

Review

Background

Strongly correlated-electron materials, such as the rare-earth perovskite oxide manganites having a general formula $R_{1-x}AxMnO_3$, where R is a trivalent rare-earth element (e.g., La, Pr, Sm) and A is a divalent alkaline-earth element such as Ca, Sr, and Ba, have been attracting much attention because of their unusual electron-transport and magnetic properties, e.g., colossal magnetoresistance (CMR) effect [1-3], a sharp metal-insulator transition (MIT) as a function

of temperature, electric field, magnetic field, light, hydrostatic pressure, strain, etc. [4-6]. Such MIT is also accompanied by a paramagnetic to ferromagnetic transition as the temperature is lowered. The competition between several interactions in the rare-earth perovskite oxide manganites makes that only small energy differences exist between the different possible phases of the system. As a result, the phase of the material can be tuned by various external perturbations, such as magnetic and electric fields, strain, and disorder. These perturbations may lead to the CMR effect and can be used for electronic phase control in manganite devices. Recently, there is strong experimental evidence to indicate that the rare-earth perovskite oxide manganites are

* Correspondence: xhzhu@nju.edu.cn

National Laboratory of Solid State Microstructures, School of Physics, Nanjing University, Nanjing 210093, China

electronically inhomogeneous, which consist of different spatial regions with different electronic orders [7-10], a phenomenon that is named as electronic phase separation (EPS). As an inherent electronic inhomogeneity, EPS has been widely reported in the rare-earth perovskite oxide manganites, and its size varies from nano to mesoscopic scales [11-15]. It has been recognized to be crucial for the CMR effect and the MIT in manganites, leading to the new applications of spintronics [9]. However, the presence of EPS raises many intriguing questions, e.g., what is the microscopic nature of the EPS? Why does it have such a large range of length scales from nanometers to micrometers? More importantly, is it responsible for the related physical properties such as CMR and high-T_c superconducting exhibited by the manganites and related oxide materials? Therefore, EPS is getting recognized as a phenomenon of importance in understanding the magnetic and electron transport properties of perovskite oxide manganites [16,17].

Recent advances in science and technology of perovskite oxide manganites have resulted in the feature sizes of the microelectronic devices based on perovskite oxide manganites entering into nanoscale dimensions. At nanoscale, perovskite oxide manganites exhibit a pronounced size effect manifesting itself in a significant deviation of the properties of low-dimensional structures from their bulk and film counterparts. For example, in the charge-ordered half-doped manganite nanoparticles, a robust charge ordering (CO) state and antiferromagnetic (AFM) ground state are significantly suppressed whereas a ferromagnetic (FM) ordering is exhibited [18-22]; meanwhile, there exists size-dependent exchange bias effect and glassy behaviors [23-26]. In the nanostructured patterns of (La, Pr,Ca)MnO₃ (LPCMO) narrow strips (spatial confined system), several new transport features such as giant resistance jumps [27-30], reentrant M-I transitions [31], negative differential resistances, and intrinsic tunneling magnetoresistance [32,33] emerge, which are absent in the thin films and bulks. Furthermore, as the geometry size of the low-dimensional manganite nanostructures is further reduced to the characteristic EPS length scale (typically several tens of nanometers in manganites), the EPS is expected to be strongly modulated, leading to quite dramatic changes in functionality and more emergent phenomena [34]. Therefore, reduced dimensionality will open a door to the new functionalities in perovskite manganites and offer a way to gain new insight into the nature of EPS in the perovskite manganite system [35]. In the recent years, much progress has been made in understanding the physical nature of the EPS in low-dimensional perovskite manganite nanostructures both from experimentalists and theorists, which have a profound impact on the manganite oxide nanoelectronics. In this work, we review the major progress of the EPS in low-dimensional

perovskite manganite nanostructures, which are based on the recent literatures about the EPS in perovskite manganite nanoparticles, nanowires/nanotubes, and nanostructured films and/or patterns. The possible physical origins of the EPS are also discussed from the signatures of electronic inhomogeneities as well as some theoretical scenarios to shed light on understanding this phenomenon. We end this review by providing our perspectives to the future research directions in this area.

Research history of EPS and its signatures

The first report on the EPS in perovskite manganites was back to 1950s, where Wollan and Koehler carried out their pioneering neutron scattering studies of La_{1-x}Ca_xMnO₃ (LCMO) [36]. They observed both FM and AFM peaks in the magnetic structure of LCMO by neutron scattering, and concluded that there is the simultaneous presence of FM and AFM phases in this material. Since that time, manganites had just begun to attract the interest of physicists. In 1950, Jonker and van Santen first reported the electrical and magnetic properties of manganites, and they found a ferromagnetic conducting phase below room temperature in La_{1-x}Ca_xMnO₃ (0.2 < x < 0.4) [37,38]. Shortly afterward, Zener, Kanamori, Goodenough, and several others established the basic theoretical framework of the EPS that scientists use today [39].

Manganites and the phase separation effects they display fell out of fashion until the 1990s. Although significant magnetoresistance effects in single-crystal La_{0.69}Pb_{0.31}MnO₃ were reported in 1969, there was no technological incentive for further pursuit [40]. What reignited manganite research was the 1994 discovery by Jin and collaborators that a several-tesla magnetic field could induce a 1,000-fold change in the resistance of a heat-treated epitaxial thin film of La_{0.67}Ca_{0.33}MnO₃ [41]. A dubbed CMR, this effect arises because the applied magnetic field drives a phase transition from an insulating paramagnet to a spin-aligned metal. Thus, as Jonker and van Santen reduced the temperature to reach the conducting spin-aligned phase, Jin and his colleagues applied a magnetic field.

Recently, Woodward et al. performed a neutron diffraction study of Nd_{0.5}Sr_{0.5}MnO₃ and found that this material first became FM at 250 K, partially transforming to an A-type AFM phase at approximately 220 K, followed by a transformation of a substantial fraction to a CE-type AFM phase at approximately 150 K [42]. Their experimental results indicate that three phases (FM metallic and CE-AFM charge-ordered phases along with an A-type AFM phase) coexist at low temperatures, and the size scale of the inhomogeneities is at least in the mesoscopic range (a few hundred nanometres or more). Sub-micrometersized phase separation involving FM and charge-ordered AFM domains with a typical size of about

0.2 μm was found in $\text{La}_{0.625-y}\text{Pr}_y\text{Ca}_{0.375}\text{MnO}_3$ by transmission electron microscopy (TEM) [5]. At the same time, by using scanning tunneling spectroscopy (STM), Fäth et al. also found the evidence of electronic inhomogeneities in $\text{La}_{0.7}\text{Ca}_{0.3}\text{MnO}_3$ below the FM transition temperature with a mesoscopic scale of about 0.2 μm , where the FM metallic domains are interspersed in insulating regions [43].

Mesoscopic phase separation with the length scale between 30 and 200 nm, arising from the comparable energies of the ferromagnetic metallic and antiferromagnetic insulating states, is just one extreme in the perovskite manganites [5]. Normally, the EPS with phases of different charge densities is expected to give rise to nanometer scale clusters because large phase separated domains would break up into small pieces due to the Coulomb interactions. For example, Mori et al. reported a nanoscopic length scale of the electronic inhomogeneity in thin films of the hole-doped side of $(\text{La,Ca})\text{MnO}_3$ by high-resolution TEM [44]. Similarly, in $\text{Bi}_{0.25}\text{Ca}_{0.75}\text{MnO}_3$, Renner et al. also found nanoscopic charge-ordered and metallic domains which were correlated with the structural distortions [45]. Generally, microscopically homogeneous clusters are usually in the diameter size of 1 to 2 nm dispersed in an insulating or charge-localized matrix. For example, recently, De Teresa et al. [46] reported on the experimental evidence for the existence of nanoscopic phase segregation in the manganite compounds of $(\text{La}_{1-x}\text{A}_x)_{2/3}\text{Ca}_{1/3}\text{MnO}_3$ ($\text{A} = \text{Y}$ or Tb), in which the spontaneous formation of localized magnetic clusters with size of ~ 1.2 nm above the ferromagnetic ordering temperature was revealed by a combination of volume thermal expansion, magnetic susceptibility, and small-angle neutron scattering measurements. These nano-sized magnetic clusters grew in size but decreased in numbers under an external applied magnetic field. Such a phase separation scenario bridges the gap between the double-exchange model and the lattice distortion models.

The signatures of EPS can be revealed by different techniques depending on the length scale on which it occurs. For mesoscopic phase separation, diffraction techniques can be used to reveal its distinct features since the size scale of the inhomogeneities is large enough to produce well-defined reflections in neutron and X-ray diffraction patterns [9]. However, for the nanoscopic electronic inhomogeneity in manganites, both TEM, high-resolution TEM and scanning transmission electron microscopy (STEM), and STM can be used to reveal the coexistence of nanoscopic charge-ordered (insulating) domains and the FM metallic domains, giving the local structural information at atomic level [5]. It is often difficult to identify EPS based on the magnetization and transport measurements because of the sensitivity of phase separation to magnetic fields. Thus, magnetic fields transform the antiferromagnetic insulating state to the ferromagnetic

metallic state. However, transport measurements, under favorable conditions, can provide valuable information on phase separation.

EPS in low-dimensional perovskite manganite nanostructures

Over the last decade, nanomaterials have received much attention from the scientific and engineering viewpoints. They exhibit different properties from those of bulk materials due to their small size and large surface-to-volume ratios, and become promising candidates for nanometer scale electronic, optical, and mechanical devices. Recent advances in science and technology of perovskite manganites have resulted in the feature sizes of perovskite manganite-based oxide electronic devices entering into nanoscale dimensions. As the spatial dimension of the low-dimensional manganite nanostructures is reduced to the characteristic EPS length scale, quite dramatic changes in their transport properties such as ultrasharp jumps of magnetoresistance, reentrant MIT, negative differential resistances, and intrinsic tunneling magnetoresistance could appear, which are believed to be caused in large part by the EPS in perovskite manganite nanostructures [27-33]. They have significant impacts on fabricating oxide-based novel devices. To better understand the EPS phenomenon in low-dimensional perovskite manganite nanostructures, in the past several years, various synthetic methods such as sol-gel technique [47], hydrothermal synthesis [48,49], electro-spinning process [50,51], template method [52-54], and lithographic techniques [27,29-31,33,34] have been developed to fabricate low-dimensional manganite nanostructures, such as manganite nanoparticles, nanowires/nanotubes, and nanostructured films/patterns. In addition, the new technologies to directly identify the EPS phenomenon in low-dimensional perovskite manganite nanostructures have been developed, such as scanning electron nanodiffraction [13], atomic-resolution STM [45], MFM [4,55], and electron holography [11]. In this section, we will review the recent progress on the EPS in low-dimensional perovskite manganite nanostructures.

EPS in manganite nanoparticles

EPS is an important phenomenon in CMR material, which leads to the new applications of spintronics. Along with the development of nanotechnology, the EPS phenomenon in CMR nanoparticles are received much attention. Recently, the evolution of the EPS with magnetic field in nanosized $\text{Nd}_{0.5}\text{Ca}_{0.5}\text{MnO}_3$ [19], $\text{La}_{0.25}\text{Ca}_{0.75}\text{MnO}_3$ [47], $\text{Pr}_{0.5}\text{Ca}_{0.5}\text{MnO}_3$ [21], $\text{La}_{0.2}\text{Ca}_{0.8}\text{MnO}_3$ [56], and $\text{Pr}_{0.67}\text{Ca}_{0.33}\text{MnO}_3$ [57] particles has been reported. For example, in nanosized $\text{Pr}_{0.67}\text{Ca}_{0.33}\text{MnO}_3$ particles with average diameter of 100 nm, it was found that a sharp transition from AFM to FM did not occur even up to 60 kOe, as demonstrated in Figure 1 [57]. The field dependence of the

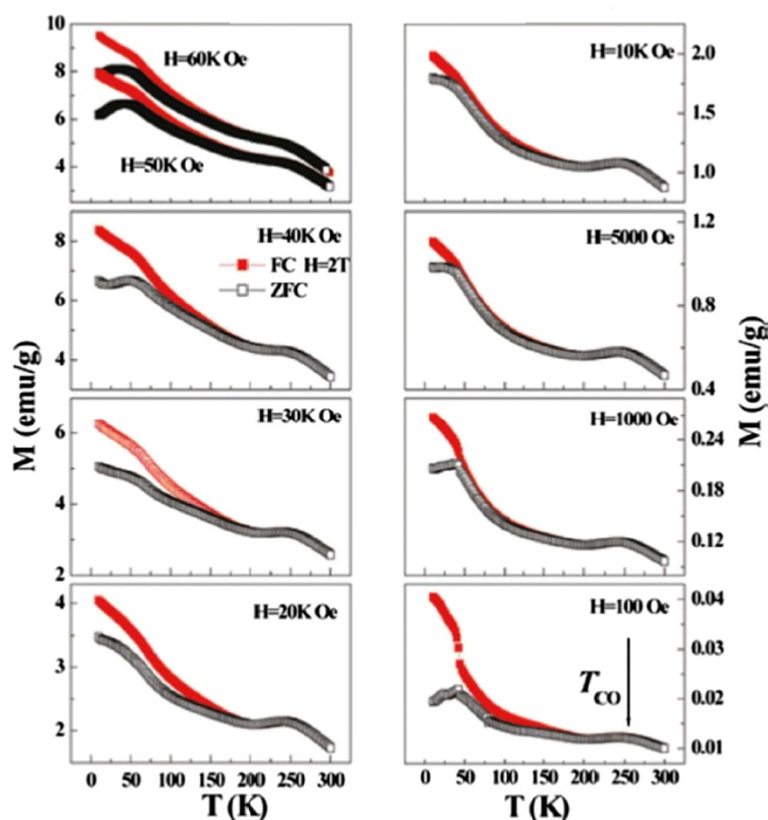
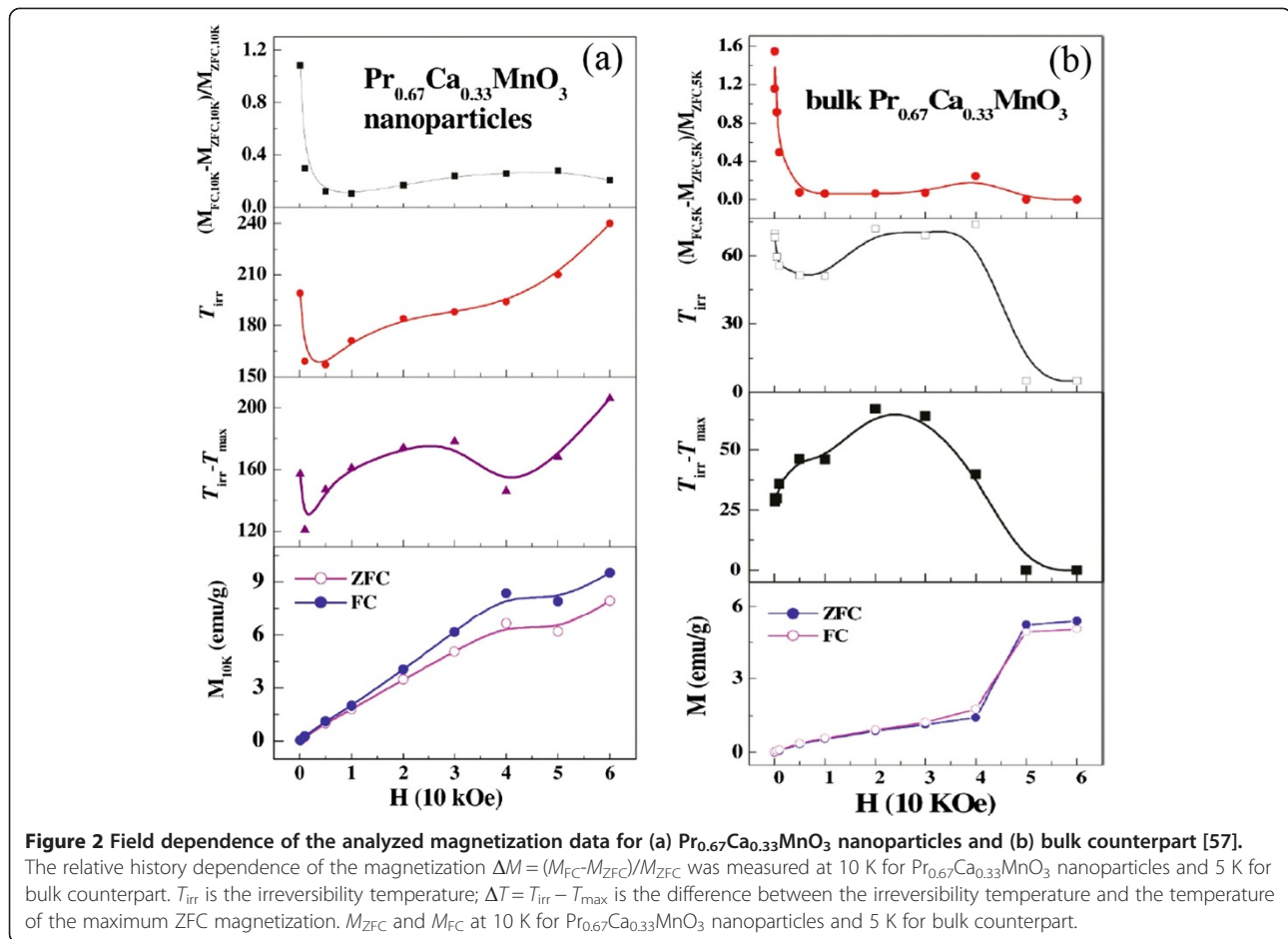


Figure 1 Field cooled and zero field cooled magnetization of $\text{Pr}_{0.67}\text{Ca}_{0.33}\text{MnO}_3$ nanoparticles. Field cooled (closed symbols) and zero field cooled (open symbols) magnetization of $\text{Pr}_{0.67}\text{Ca}_{0.33}\text{MnO}_3$ nanoparticles as a function of temperature, measured in the field ranges from 100 Oe to 60 kOe [57].

analyzed magnetization data for the $\text{Pr}_{0.67}\text{Ca}_{0.33}\text{MnO}_3$ nanoparticles is shown in Figure 2 [57]. As a comparison, the data for the bulk counterpart is also given out. It is clear that the evolution trend of ΔM is a little different from that of the bulk counterpart, i.e., first a sharp decrease and then an increase slowly up to 50 kOe. However, the irreversibility temperature (T_{irr}) exhibits a very different change trend as compared with that of the bulk counterpart, which is sharply decreased from 100 to 5,000 Oe and then continually increased. The magnetization M_{ZFC} and M_{FC} are increased smoothly with increasing the magnetic field H up to 60 kOe but a step-like increase of M_{ZFC} and M_{FC} like in bulk counterpart is not observed. For H below 5,000 Oe, the first sharp decrease of the ΔM , T_{irr} and weak decline of ΔT is attributed to the gradual conquest of the anisotropy of frozen spin and alignment with field, since the magnetic field is not large enough to induce the growth of the FM cluster. Due to the surface effect, the FM-like surface spins contribute additional moment, which leads to a large magnetization for nanoparticles as compared with bulk counterpart. However, due to the strong coupling between the surface spins and interface spins (which

also deviate from AFM arrangement), the exchange field required to force a transition of surface spins and interface spins to full FM is approximately 5×10^6 Oe [58]. As a consequence, even the field is increased up to 60 kOe, which can align the AFM core spins like for bulk, it is still not large enough to make the nanoparticles to be full FM configuration, thus leading to a slow increase of the ΔM and T_{irr} [58]. The significant increase of the exchange bias field of the $\text{Pr}_{0.67}\text{Ca}_{0.33}\text{MnO}_3$ nanoparticle as compared with the bulk counterpart can be attributed to the surface pressure and uncompensated surface spins.

Recently, the EPS in $\text{La}_{0.7}\text{Sr}_{0.3}\text{MnO}_3$ nanoparticles synthesized by sol-gel process was also investigated by electron magnetic resonance (EMR) method [59]. The results showed that all the $\text{La}_{0.7}\text{Sr}_{0.3}\text{MnO}_3$ nanoparticles (synthesized with different gelation agents) exhibited the following common features: (i) at the PM region, the EMR line was pure Lorentzian having a g value decreasing with increasing the temperature and g value reached 2 at around 350 K; (ii) when the temperatures are crossing T_c , the EMR lines changed their resonance fields (e.g., lineshapes and linewidths); (iii) all samples showed the coexistence of FM and PM signals within a wide temperature range

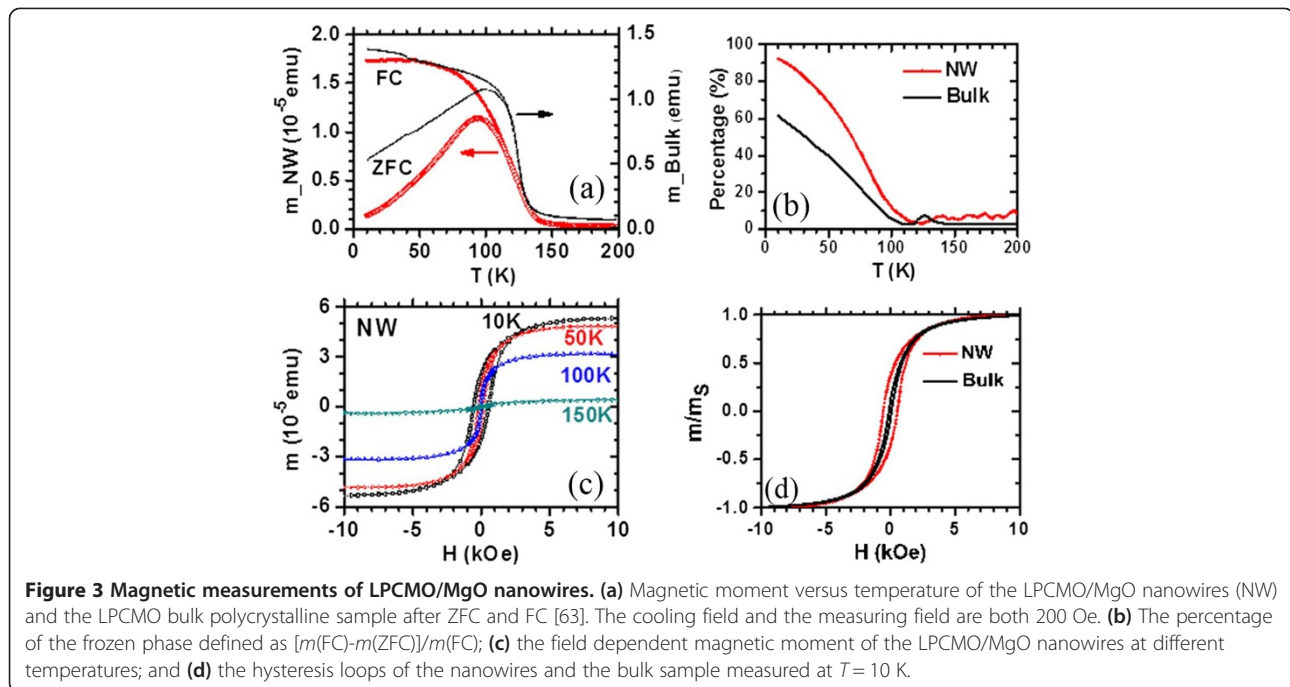


below T_c ; and the intensity of PM signal increased gradually as the temperature approached to T_c . The growth of PM phase was accompanied by a consequent decrease of FM signal intensity. Besides these common features, the EMR spectra of the measured samples also show several significant differences, which allow ones to investigate the origin of PS in these samples. It was found that the $\text{La}_{0.7}\text{Sr}_{0.3}\text{MnO}_3$ nanoparticles synthesized with different gelation agents in sol-gel process exhibited different magnetic behaviors, and a sharp FM-PM transition was observed in the $\text{La}_{0.7}\text{Sr}_{0.3}\text{MnO}_3$ nanoparticles synthesized with a combined agent of urea and trisodium citrate. These results also demonstrate that the synthesis conditions of perovskite manganite nanoparticles have an important role in their microstructure, magnetic properties, and phase separation behavior.

EPS in manganite nanowires/nanotubes

One-dimensional manganite nanostructures that include nanowires, nanorods, and nanotubes have attracted rapidly growing interest due to their fascinating electrical and magneto-transport properties. They are emerging as important building blocks serving as interconnects and

active components in nanoscale electronic, magnetic, and spintronic devices. It is expected that the manganite nanowires will exhibit an emerging magnetic and transport behaviors associated the EPS due to the strong electronic correlation under a spatial confinement in the case of nanowires [35]. Recently, theoretical calculations using the FM Kondo Hamiltonian have predicted that the intrinsic EPS persists in one-dimensional manganite nanostructures [60]. However, due to the growth difficulty in single-crystalline manganite nanowires, the EPS in manganite nanowires are not completely explored. Recently, it has been demonstrated that by utilizing MgO nanowires as the template one can grow the transition metal oxide core-shell nanowires with good single crystalline quality [61,62]. By the same method, Li et al. synthesized the single-crystalline $\text{La}_{0.33}\text{Pr}_{0.34}\text{Ca}_{0.33}\text{MnO}_3$ (LPCMO)/MgO core-shell nanowires with diameters about tens of nanometers [63]. Their structure and morphology characterizations confirm the epitaxial growth of $\text{La}_{0.33}\text{Pr}_{0.34}\text{Ca}_{0.33}\text{MnO}_3$ shell layers on MgO core layers. The magnetic measurements are shown in Figure 3 [63]. As shown in Figure 3a, the ZFC curve and the FC curve of the LPCMO nanowires are split at a blocking temperature of



$T_b = 93$ K when the temperature is decreased. Such a ZFC/FC deviation is very similar to that of the bulk polycrystalline LPCMO sample also shown in Figure 3a, and is due to the frozen of the magnetic moment. The differences between the ZFC and FC magnetic moments in the nanowire, defined as the frozen phase magnetic moment, is significantly larger than that in the bulk counterpart below the blocking temperature sample, as shown in Figure 3b. In bulk or thin film LPCMO, the frozen phase is generally regarded to be related to the phase competition between the FM metallic phase and the AFM-CO phase [64]. So, in the nanowires, the increased amount of frozen phase concentration could be reasonable due to the stronger phase competition in the low-dimensional system. Figure 3c,d displays the magnetic field dependence of the magnetic moments of the LPCMO nanowires and the bulk counterpart. As observed in Figure 3c both the saturation magnetic moment m_s and the coercivity H_c in the LPCMO nanowires were increased as the temperature was decreased, which was similar to that in bulk or thin-film manganites. However, the differences between the nanowire and the bulk sample were also observed. The H_c value of the LPCMO nanowires was much larger than that of the LPCMO bulk sample. For example, at $T = 10$ K, H_c is about 550 Oe in the nanowire but only about 100 Oe in the bulk sample as shown in Figure 3d. The larger H_c in the nanowires could be attributed to their stronger domain wall pinning at the boundaries of the separated AFM and FM phases caused by the EPS in the nanowires [65]. These observations suggest that the EPS with a stronger phase competition exists in the one-dimensional structure.

To better understanding the role of EPS in the emergent transport behaviors of manganite one-dimensional structures, some manganite wires are also fabricated from single thin film by optical lithography, where the width of the manganite wires is reduced to a scale on the order of the inherent phase separation. As one example, LPCMO is chosen as a representative model system due to its sub-micrometer scale phase separation that can be easily accessed by conventional lithographic fabrication processes. It is found that by reducing a single-crystal LPCMO thin film to a wire with a width comparable to a scale on the order of the inherent EPS, the system exhibits ultrasharp jumps in resistivity, as shown in Figure 4 [27]. These jumps are attributed to a reduction of the transport lanes to a single channel. As the insulating barriers of the charge-ordered state are broken by the reduction of temperature or an increase in magnetic field, the resistance in the wire shows sharp jumps around the MIT, which reflects the nature of the first-order phase transition between ferromagnetic metal and charge-ordered insulator domains. Since the transport measurement can reveal the signature of phase transition of an individual EPS domain in a manganite wire, it becomes possible to probe the EPS domain dynamics of manganites. This is accomplished by setting an LPCMO wire at or very near the critical point of phase transition and measuring the phase fluctuation with high-time resolution. The very limited number of EPS domains that can be hosted in the wire effectively removes the problems associated with spatial averaging methods in the conventional transport measurements while allowing for a high

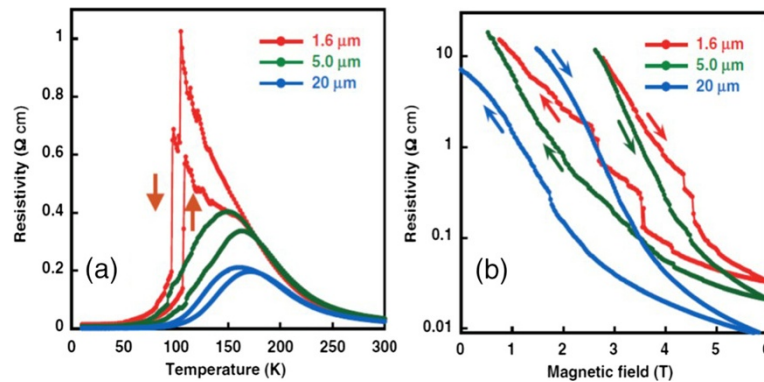


Figure 4 Resistivity versus temperature curves and resistivity vs. magnetic field curves. (a) Resistivity versus temperature (R-T) curves for the LPCMO wires under a 3.75-T magnetic field [27]. Arrows indicate the direction of the temperature ramp. The R-T curves all exhibit hysteresis behavior in cooling-warming cycles, which is consistent with the coexistence of ferromagnetic metal and charge-ordered insulator domains in the LPCMO system. The MIT is rather smooth for both the 20- μm and the 5- μm wires. Ultrasharp and giant steps are clearly visible for the 1.6- μm wire. (b) Resistivity vs. magnetic field curves for the LPCMO wires measured at 110 K. Sudden step-like jumps are again visible in the 1.6- μm wire. Arrows indicate the sweeping directions of the magnetic field for each curve.

temporal resolution. At the critical point of the MIT, single-domain fluctuations will show a clear signature in time-dependent resistivity measurements, as shown in Figure 5 [29]. In Figure 5a, the resistivity (ρ) of a 10 $\mu\text{m} \times 50 \mu\text{m} \times 70 \text{ nm}$ LPCMO wire under a 3.75-T magnetic field exhibits an ultrasharp jump at the MIT centered at 83 K. This is contrasted with the same sample in a film geometry (Figure 5a, inset) which shows a smooth transition from metallic to insulating behavior across a 150-K window. The extremely large jump in the resistivity of the wire results solely from its geometry's ability to remove the effects of spatial averaging in transport measurements. By setting the temperature of the LPCMO wire precisely in the middle of the 2-K window found in the temperature-dependent resistivity scan, it is possible to study the microscopic details of the transition in both space and time. Figure 5b shows the time-dependent resistivity while the wire is held at the transition temperature. It is clear that the apparent two-state system with resistivity jumps is actually comprised of a much richer multistate system. There are three inherent resistivity levels, each containing a further two-state

fluctuation. However, in unconfined structures such as film (inset in Figure 5) or bulk counterpart, only white noise is observed. These data clearly show that the fluctuations that change the electrical resistance exist in these phase-separated manganite wires. It is observed that these fluctuations exist only near the transition temperature where electronic domains are fluctuating between FMM and COI and are not individually observable in films or bulk transport experiments. Therefore, the fluctuations in the wire are the direct signal of the microscopic fluctuations in EPS domains at the transition temperature. The comparable dimensions of the inherent domains to the wire result in a large change in the total wire resistance when a single domain fluctuates from one phase to another. Not only did these findings give us new insights into the mechanisms that drive electronic phase transitions, but they also open the door to engineering novel devices and could be applied as an on-chip digital randomizer as one example. Recently, large aspect-ratio (length-to-width >300) single-crystal nanowires of $\text{La}_{2/3}\text{Ca}_{1/3}\text{MnO}_3$ were also fabricated by combined optical and focused ion beam lithographies,

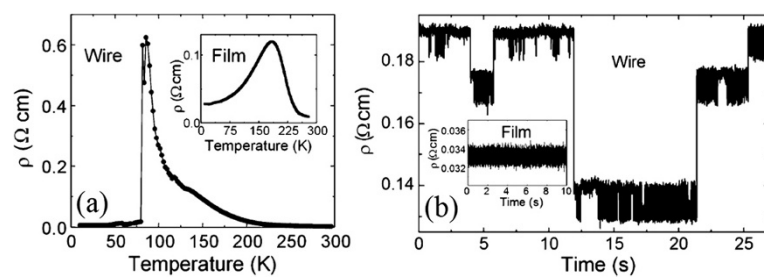


Figure 5 Time-dependent resistivity measurements. (a) Wire shows abrupt drop in resistivity at the MIT transition while the film shows a smooth transition (inset) [29]. (b) Resistivity of a wire when held at the transition temperature shows clear jumps associated with single electronic domain fluctuations. This behavior is not observed in the film, which only exhibits white noise (inset).

which preserved their functional properties [66]. Remarkably, an enhanced magnetoresistance value of 34 % in an applied magnetic field of 0.1 T in the narrowest 150-nm nanowire was obtained. Such behavior is ascribed to the strain release at the edges together with a destabilization of the insulating regions. This opens new strategies to implement these structures in functional spintronic devices.

In addition to the manganite nanowires, the EPS in the manganite nanotubes are also investigated. Nanotubes are different from nanowires because they typically have a hollow cavity, whereas nanowires are completely filled with nanomaterials. From a viewpoint of device engineering and theoretical considerations, manganite nanotubes with nonplanar geometries have a variety of applications for nanoelectronic components [67-69], transducers, or sensors [70,71]. Recently, perovskite rare-earth manganese tubes such as $\text{La}_{0.67}\text{Sr}_{0.33}\text{MnO}_3$ (LSMO), $\text{La}_{0.67}\text{Ca}_{0.33}\text{MnO}_3$ (LCMO), and $\text{La}_{0.325}\text{Pr}_{0.300}\text{Ca}_{0.375}\text{MnO}_3$ (LPCMO) have been fabricated using a sol-gel template synthesis process [53,72,73]. Their typical length is about 6 to 8 μm and the average wall thickness is 45, 60, and 150 nm for LSMO, LCMO, and LPCMO, respectively [54]. The walls of the tubes are composed of magnetic nanograins, and their sizes are less than the critical size for multidomain formation in manganites. As a consequence, each particle that constitutes the nanotube walls is a single magnetic domain. Figure 6a shows the magnetizations of the LSMO, LCMO, and LPCMO nanotubes as a function of the temperature T measured at different applied magnetic fields (only show the data measured at $H = 100$ Oe) following the next protocol: zero-field cooling (ZFC) (1 in Figure 6a), cooling the sample from the highest T with $H = 0$ Oe; afterward, a magnetic field of $H = 100$ Oe was applied and the magnetization data were collected increasing T . Field cool cooling (FCC) (2 in Figure 6a) is performed by measuring the magnetization by cooling the

sample with $H = 100$ Oe [54]. Finally, in field cool warming (FCW) (3 in the same plot), the system is warmed with $H = 100$ Oe after FCC. It was noticed that there exists differences between the FCC (2*) and FCW (3*) curves in a broad temperature range for LPCMO nanotubes. Figure 6b displays the square-root temperature dependence of the coercive fields for the LSMO, LSMO, and LPCMO nanotubes [54]. Clearly, the coercive fields of the LSMO and LSMO nanotubes followed a linear dependence with the square root of temperature, whereas a nonlinear dependence was observed in LPCMO nanotubes, and the higher coercive field value was associated with the competition between the CO and the FM phases in the phase separated LPCMO nanotubes. Normally, a linear dependence is expected in the noninteracting particle systems, which can originate in the single magnetic domains that constitute the walls of the ferromagnetic nanotubes [74]. Therefore, as shown in Figure 6, the LSMO and LCMO nanotubes present a homogeneous ferromagnetic behavior below 340 and 258 K, respectively. The magnetic dead layer avoids the exchange interaction between the nanograins, but the dipolar interaction between them was detected which suggests a fanning array of magnetic moments along the tube axis. The coercive field temperature dependence indicates the presence of weak interactions. As for the LPCMO nanotubes, they became mainly ferromagnetic below 200 K. Their thermal hysteresis and the low magnetization values indicate the presence of an extra charge-ordered phase in the LPCMO nanotubes. The small grain size may generate small charge-disordered regions, which are easily transformed to a ferromagnetic region by field or increasing/decreasing temperature. Also, the charge-disordered phase attenuates the interaction between single magnetic domains when this phase is reduced by the application of a magnetic field; the system increases its ferromagnetic character. So, the control of the charge-disordered phase fraction

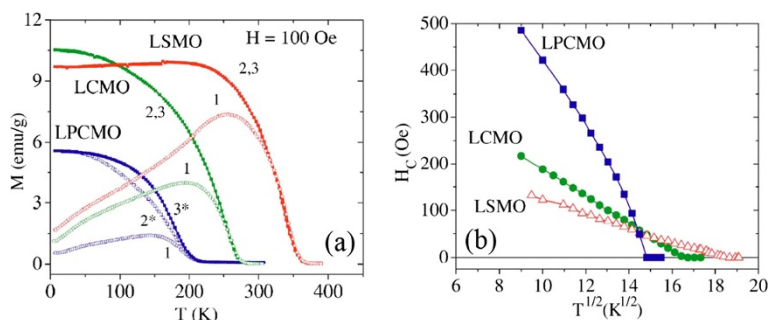


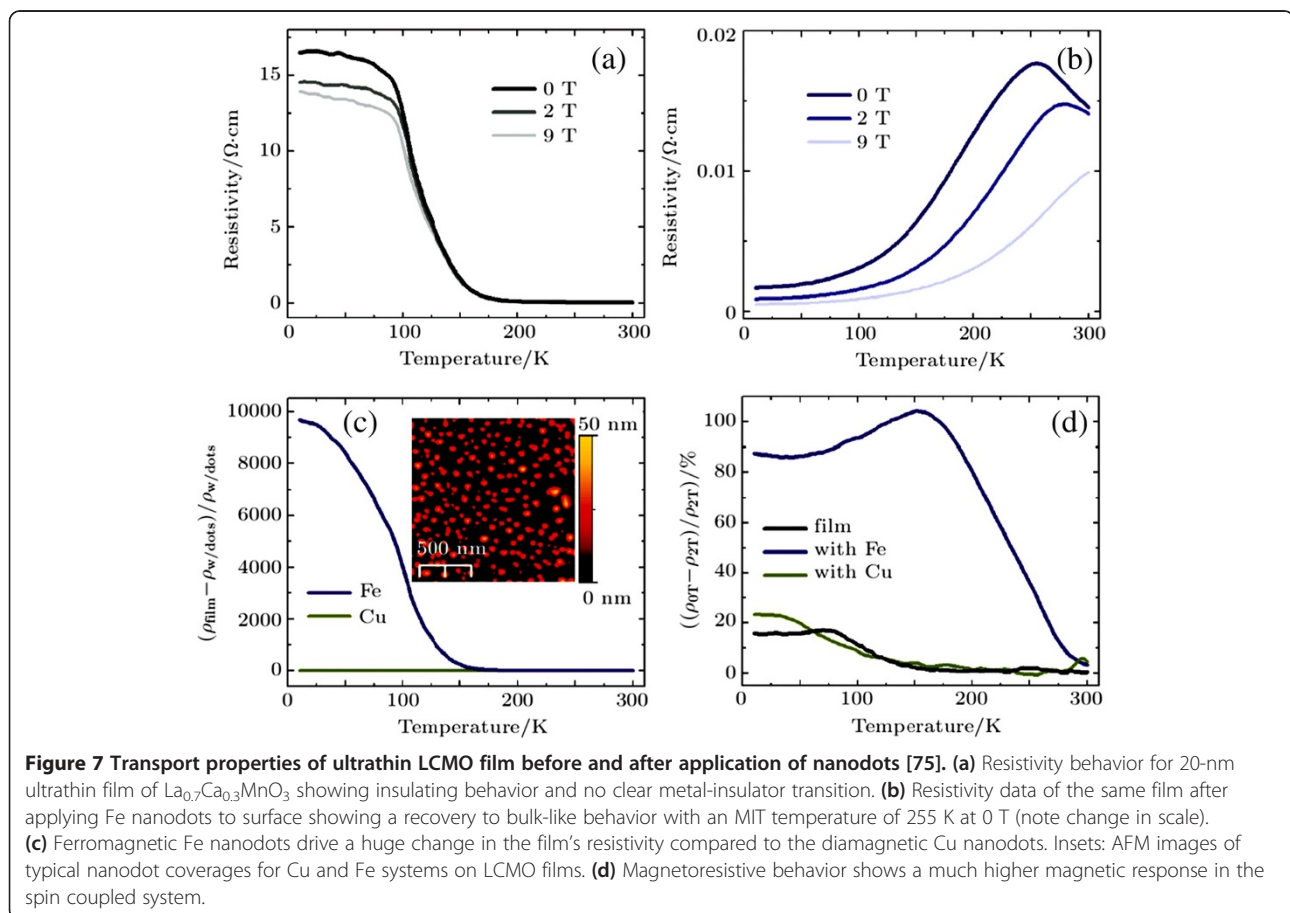
Figure 6 Magnetizations and square-root temperature dependence of the LSMO, LCMO, and LPCMO nanotubes. (a) M vs T at 100 Oe of LSMO, LCMO, and LPCMO nanotubes after different magnetothermal processes [54]. The numbers 1, 2, and 3 show the data collected in a 1 ZFC warming process after cooling with zero magnetic field, 2 FCC cooling process with a magnetic applied field of 100 Oe, and 3 FCW warming after the FCC process with 100 Oe. The asterisk indicates that the FCC and FCW in the LPCMO-nanotubes are different. **(b)** Square-root temperature dependence of the coercive fields for the LCMO, LSMO, and LPCMO nanotubes.

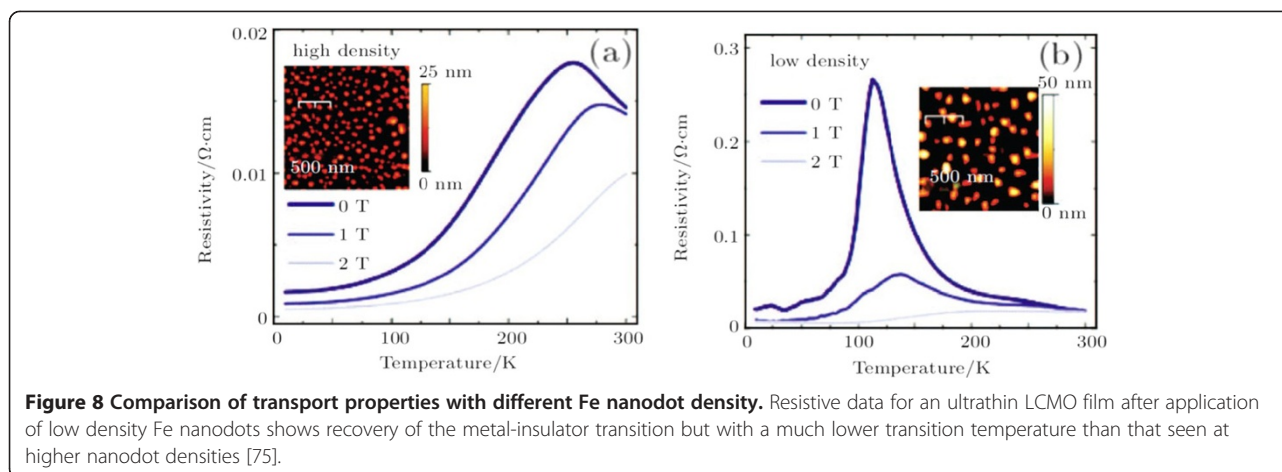
could be used to tune the magnitude of the interaction between the single magnetic domains which affects the coercive fields.

EPS in manganite nanostructured films/patterns

In most CMR manganites, both the MIT and the amplitude of magnetoresistance are critically dependent upon the percolation of ferromagnetic metal domains in the system. Controlling the formation and the spatial distribution (size, density, symmetry, etc.) of the electronic domains will not only help to understand the origin of the EPS but also help to design manganites or other correlated electronic materials with desired properties for all-oxide-based electronic devices. Recently, a novel method called electronic nanofabrication (a conceptually new approach) is developed to control the formation and the spatial distribution of electronic domains in manganites [35]. In contrast to the conventional nanofabrication, the electronic nanofabrication patterns electronic states in materials without changing the actual size, shape, and chemical composition of the materials, which is a promising method for manganites. For example, magnetic Fe nanodots are grown on the surface of a 20-nm-thick $\text{La}_{0.7}\text{Ca}_{0.3}\text{MnO}_3/\text{LaAlO}_3(001)$ film, which

could turn the film from an insulator to a metal with a high MIT temperature, as shown in Figure 7 [75]. The underlying mechanism is understood to be the local magnetic exchange field between Fe and Mn spins that aligns the local Mn spins leading to the formation of a local metallic state. As shown in Figure 8, the MIT temperature can be also tuned by the density of Fe nanodots, which strongly indicates that the local metallic state follows the spatial locations of the Fe nanodots [75]. Besides the electronic nanofabrication technique, other methods such as atomic force microscopy lithography [28], electron-beam lithography (EBL) [76-80], focused ion beam (FIB) milling [33,34,81-84], and chemical growth and etching [85,86] are also used to fabricate manganite nanostructured patterns from oxide thin films. For example, microscopic $\text{Pr}_{0.65}(\text{Ca}_{0.75}\text{Sr}_{0.25})_{0.35}\text{MnO}_3$ (PCSMO) thin films were fabricated into patterns by EBL with width comparable to the length scale of EPS ($\sim 1 \mu\text{m}$), where spontaneous resistance jumps along with the local Joule heating-induced step-like negative differential resistance were clearly observed [76]. Recently, LCMO microbridges with different widths were also fabricated by EBL method, where the MIT temperature was found to be decreased as reducing the bridge width, and the MIT even disappeared over



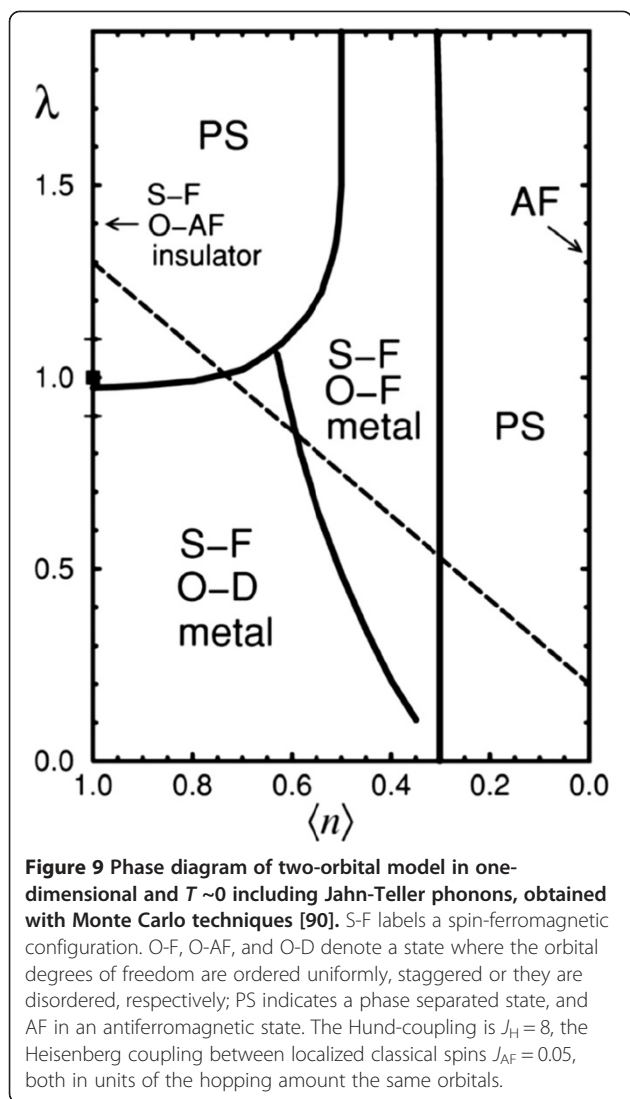


the measured temperature range for the bridge with a width of 500 nm [76]. The underlying mechanism for this phenomenon is the confined geometry, which is dominated by the filamentary conduction mechanism. The magnetoresistance of the bridge also shows interesting behavior for enhanced e - e interactions in the presence of spin disorder; it can decrease and even change its sign in the bridges with widths of 1.5 and 1.0 μm under magnetic field of 1 T. The obvious size effects in the manganite microbridge nanopatterns are invaluable for further understanding the EPS phenomenon and its role in CMR effect.

Origin of EPS in perovskite manganite nanostructures

EPS as an inherent electronic inhomogeneity has been observed in real space with atomic-scale resolution in the perovskite manganites, which is generally regarded to be crucial for the CMR effect. This greatly stimulates a growing and theoretical interest in the EPS of perovskite manganite nanostructures. Now, the main theoretical approaches developed for investigating the EPS in perovskite manganite nanostructures can be classified into two categories, namely, approaches based on the model Hamiltonians and phenomenological theory. Dagotto and colleagues have developed one-orbital FM Kondo model and two-orbital model with Jahn-Teller phonons to investigate the EPS phenomenon in one-dimensional manganites [58,87-89]. In the model of Kondo lattice Hamiltonian with ferromagnetic Hund's coupling, the classical limit for the spin of the (localized) t_{2g} electrons is analyzed on lattices of dimension 1, 2, 3, and ∞ using several numerical methods [60,87,88]. They found that the expected double-exchange-induced strong tendencies to ferromagnetic correlations at low temperatures were in competition with a regime of phase separation, which occurred between the hole-undoped antiferromagnetic and hole-rich ferromagnetic regions. Although, the one-orbital model for manganites contains interesting

physics, notably, a FM-AF competition that has similarities with those found in experiments. However, to explain the notorious orbital order tendency in Mn-oxides, it is crucial to use a model with two orbitals, where there is an electron Jahn-Teller phonon coupling and also Coulomb interactions [89,90]. Under the assumption that both localized e_g -spins and phonons are classical, the model without Coulombic terms can be studied fairly accurately using numerical and mean-field approximations. The calculated results for a one-dimensional system at low temperature by considering the two e_g orbitals and the Jahn-Teller phonons enrich the phase diagram considerably, as shown in Figure 9 [90]. Obviously, the phase diagram is much rich, which includes different phases such as metallic and insulating regimes with orbital order. It is clear that phase separation appears at small e_g -densities between an electron-undoped AF-state and a metallic uniform-orbital-ordered FM state. Ahn et al. also proposed a model Hamiltonian including electron-phonon interactions and long-range elastic coupling between the local lattice distortions [91]. They presented a scenario for mesoscopic/microscopic inhomogeneities and suggested them to be the main source of the CMR effect. Since the physics of perovskite manganites is controlled by many degrees of freedom at the atomic level and the associated energy scales, Ramakrishnan et al. also developed a microscopic model for manganites that includes all the important energy scales present in them [92]. In this model, the degeneracy of the two e_g orbitals is split into two types of states, l and b at each manganese site by electron-lattice coupling. The l state is polaronic and has an exponentially reduced hopping amplitude, whereas the electrons within the b states hop with the bare amplitude. Such two-fluid model of manganites demonstrates colossal magnetoresistive response and reproduces the physical transport properties confirmed by the experimental measurements. Due to the local strong Mott-Hubbard repulsion, the simultaneous occupation at



both the l and b states on a given site is not allowed; this model exhibits macroscopic phase separation, where the region with l polarons corresponds to the charge-ordered states, while that with b electrons corresponds to the FM metal. However, due to the frustration of the long-range Coulomb interactions, the phase separation usually exhibits as a structure of nanoscopic FM metallic domains with interspersed domains of polaron Coulomb glass, similar to the charge-ordered FM state revealed by the electron holography [11]. Therefore, the manganites are intrinsically inhomogeneous at length scales of nanometers due to the strong electronic correlations. A phenomenological Ginzburg-Landau theory approach is also developed by using a Landau free-energy function and introducing the term of electronic softness to rationalize the possibility of phase coexistence and electronic inhomogeneities [93]. In this approach, magnetic and charge

modulations are argued to coexist in new thermodynamic phases in contrast to the previous models where the phase separation originates from disorder or as a strain-induced kinetic phenomenon. This approach leads to a rich diagram of equilibrium phases, qualitatively similar to those seen experimentally. The success of this approach argues for a fundamental reinterpretation of the nature of charge modulation in manganite materials, from a localized to a more extended 'charge-density wave' picture. The same symmetry considerations that favor textured coexistence of charge and magnetic order may apply to many electronic systems with competing phases. The resulting 'electronically soft' phases of matter with incommensurate, inhomogeneous, and mixed order may be general phenomena in correlated systems.

Since a number of competing energy scales are operative in manganite oxides giving rise to a large number of electronic orders such as spin, charge, and orbital (and associated lattice order), the emergence of these orders and the associated couplings between them should be considered in a full Hamiltonian model for manganites, which makes the theoretical understanding of the EPS quite complex. Much work is further needed in this challenging area of research.

Conclusions

In recent years, a remarkable progress has been achieved in understanding the EPS phenomenon in low-dimensional perovskite manganite nanostructures such as manganite nanoparticles, nanowires, nanotubes, and nanostructured films/patterns. This progress is mainly made possible by building upon the experimental measurements and theoretical approaches, and clearly establishes the phase completion as the main source of the CMR effect in manganite oxides. The shape and scale of EPS are different for different systems with electronic domain sizes ranging from a few nanometers to several micrometers. However, the microscopic nature of the EPS in perovskite manganite oxides and the physical origin of the large length-scales that arise in these systems are still unclear although much theoretical work based on model Hamiltonians and phenomenological models has been done. Clearly, much further work is needed to be done on both the experimental and theoretical fronts to understand the nature of the EPS manganite oxides, especially at the nanoscale. On the experimental side, a new technique is needed to be developed to control the formation and the spatial distribution of electronic domains in manganite oxides, which should allow to simultaneously probe EPS domains with different electronic states and give the vital information on phase formation, movement, and fluctuation. Such a novel technique called electronic nanofabrication has been developed. In striking contrast to the conventional nanofabrication, the

electronic nanofabrication patterns electronic states in materials without changing the actual size, shape, and chemical composition of the materials, which allows one to control the global physical properties of the system at a very fundamental level and greatly enhances the potential for realizing true oxide electronics. The theorists need to quantitatively clarify the electronic properties of the various manganite phases based on microscopic Hamiltonians, including strong electron–phonon Jahn–Teller and/or Coulomb interactions. Thus, quantitative calculations for addressing the CMR effect help us to better understand the physical nature of EPS phenomenon. However, to get a full understanding of the EPS phenomenon in low-dimensional manganite nanostructures, much work remains to be done for realizing its practical applications in oxide electronics.

Competing interests

The authors declare that they have no competing interests.

Authors' contributions

LL and XZ designed the structure and modified the manuscript articles; LL drafted the manuscript. HW participated in the sequence alignment. All authors read and approved the final manuscript.

Acknowledgements

This work was partially supported by National Natural Science Foundation of China (Grant Nos. 11174122 and 11134004), National Basic Research Program of China (Grant Nos. 2009CB929503 and 2012CB619400), and the open project from National Laboratory of Solid State Microstructures, Nanjing University.

Received: 27 May 2014 Accepted: 23 June 2014

Published: 28 June 2014

References

- Schiffer P, Ramirez AP, Bao W, Cheong SW: Low temperature magnetoresistance and the magnetic phase diagram of $\text{La}_{1-x}\text{Ca}_x\text{MnO}_3$. *Phys Rev Lett* 1995, **75**:3336.
- Salamon MB, Jaime M: The physics of manganites: structure and transport. *Rev Mod Phys* 2001, **73**:583.
- Dagotto E: Complexity in strongly correlated electronic systems. *Science* 2005, **309**:257.
- Zhang L, Israel C, Biswas A, Greene RL, de Lozanne A: Direct observation of percolation in a manganite thin film. *Science* 2002, **298**:805.
- Uehara M, Mori S, Chen CH, Cheong SW: Percolative phase separation underlies colossal magnetoresistance in mixed-valent manganites. *Nature* 1999, **399**:560.
- Asamitsu A, Tomioka Y, Kuwahara H, Tokura Y: Current switching of resistive states in magnetoresistive manganites. *Nature* 1997, **388**:50.
- Mathur ND, Littlewood PB: Mesoscopic texture in manganites. *Phys. Today* 2003, **56**:25.
- Rao CNR, Kundu AK, Seikh MM, Sudheendra L: Electronic phase separation in transition metal oxide systems. *Dalton Trans* 2004, **19**:3003.
- Dagotto E, Hotta T, Moreo A: Colossal magnetoresistant materials: the key role of phase separation. *Phys Rep* 2001, **344**:1.
- Shenoy VB, Gupta T, Krishnamurthy HR, Ramakrishnan TV: Coulomb interactions and nanoscale electronic inhomogeneities in manganites. *Phys Rev Lett* 2007, **98**:097201.
- Loudon JC, Mathur ND, Midgley PA: Charge-ordered ferromagnetic phase in $\text{La}_0.5\text{Ca}_0.5\text{MnO}_3$. *Nature* 2002, **420**:797.
- Ma JX, Gillaspie DT, Plummer EW, Shen J: Visualization of localized holes in manganite thin films with atomic resolution. *Phys Rev Lett* 2005, **95**:237210.
- Tao J, Niebieskikwiat D, Varela M, Luo W, Schofield MA, Zhu Y, Salamon MB, Zuo JM, Pantelides ST, Pennycook SJ: Direct imaging of nanoscale phase separation in $\text{La}_0.55\text{Ca}_0.45\text{MnO}_3$: relationship to colossal magnetoresistance. *Phys Rev Lett* 2009, **103**:097202.
- Murakami Y, Kasai H, Kim JJ, Mamishin S, Shindo D, Mori S, Tomomura A: Ferromagnetic domain nucleation and growth in colossal magnetoresistive manganite. *Nat Nanotech* 2010, **5**:37.
- Lai KJ, Nakamura M, Kundhikanjana W, Kawasaki M, Tokura Y, Kelly MA, Shen ZX: Mesoscopic percolating resistance network in a strained manganite thin film. *Science* 2010, **329**:190.
- Shenoy VB, Sarma DD, Rao CNR: Electronic phase separation in correlated oxides: the phenomenon, its present status and future prospects. *ChemPhysChem* 2006, **7**:2053.
- Shenoy VB, Rao CNR: Electronic phase separation and other novel phenomena and properties exhibited by mixed-valent rare-earth manganites and related materials. *Phil Trans R Soc A* 2008, **366**:63.
- Rao SS, Anuradha KN, Sarangi S, Bhat SV: Weakening of charge order and antiferromagnetic to ferromagnetic switch over in $\text{Pr}_0.5\text{Ca}_0.5\text{MnO}_3$ nanowires. *Appl Phys Lett* 2005, **87**:182503.
- Rao SS, Tripathi S, Pandey D, Bhat SV: Suppression of charge order, disappearance of antiferromagnetism, and emergence of ferromagnetism in $\text{Nd}_{0.5}\text{Ca}_{0.5}\text{MnO}_3$ nanoparticles. *Phys Rev B* 2006, **74**:144416.
- Sarkar T, Ghosh B, Raychaudhuri AK, Chatterji T: Crystal structure and physical properties of half-doped manganite nanocrystals of less than 100-nm size. *Phys Rev B* 2008, **77**:235112.
- Zhang T, Dressel M: Grain-size effects on the charge ordering and exchange bias in $\text{Pr}_{0.5}\text{Ca}_{0.5}\text{MnO}_3$: The role of spin configuration. *Phys Rev B* 2009, **80**:014435.
- Jiráček Z, Hadová E, Kaman O, Křížek K, Maryško M, Pollert E, Dlouhá M, Vrátilav S: Ferromagnetism versus charge ordering in the $\text{Pr}_{0.5}\text{Ca}_{0.5}\text{MnO}_3$ and $\text{La}_{0.5}\text{Ca}_{0.5}\text{MnO}_3$ nanocrystals. *Phys Rev B* 2010, **81**:024403.
- Markovich V, Fita I, Wisniewski A, Jung G, Mogilyansky D, Puzniak R, Titelman L, Gorodetsky G: Spin-glass-like properties of $\text{La}_{0.8}\text{Ca}_{0.2}\text{MnO}_3$ nanoparticles ensembles. *Phys Rev B* 2010, **81**:134440.
- Markovich V, Fita I, Wisniewski A, Mogilyansky D, Puzniak R, Titelman L, Gorodetsky G: Size-driven magnetic transitions in $\text{La}_{1/3}\text{Ca}_{2/3}\text{MnO}_3$ nanoparticles. *J Appl Phys* 2010, **108**:063918.
- Huang XH, Ding JF, Zhang GQ, Hou Y, Yao YP, Li XG: Size-dependent exchange bias in $\text{La}_{0.25}\text{Ca}_{0.75}\text{MnO}_3$ nanoparticles. *Phys Rev B* 2008, **78**:224408.
- Markovich V, Fita I, Wisniewski A, Mogilyansky D, Puzniak R, Titelman L, Martin C, Gorodetsky G: Size effect on the magnetic properties of antiferromagnetic $\text{La}_{0.2}\text{Ca}_{0.8}\text{MnO}_3$ nanoparticles. *Phys Rev B* 2010, **81**:094428.
- Zhai HY, Ma JX, Gillaspie DT, Zhang XG, Ward TZ, Plummer EW, Shen J: Giant discrete steps in metal-insulator transition in perovskite manganite wires. *Phys Rev Lett* 2006, **97**:167201.
- Yanagisawa Y, Tanaka H, Kawai T, Pellegrino L: Digitalized magnetoresistance observed in $(\text{La}, \text{Pr})\text{MnO}_3$ nanochannel structures. *Appl Phys Lett* 2006, **89**:253121.
- Ward TZ, Zhang XG, Yin LF, Zhang XQ, Liu M, Snijders PC, Jesse S, Plummer EW, Cheng ZH, Dagotto E, Shen J: Time-resolved electronic phase transitions in manganites. *Phys Rev Lett* 2009, **102**:087201.
- Ward TZ, Gai Z, Guo HW, Yin LF, Shen J: Dynamics of a first-order electronic phase transition in manganites. *Phys Rev B* 2011, **83**:125125.
- Ward TZ, Liang S, Fuchigami K, Yin LF, Dagotto E, Plummer EW, Shen J: Reemergent metal-insulator transitions in manganites exposed with spatial confinement. *Phys Rev Lett* 2008, **100**:247204.
- Wu JC, Sun H, Da HX, Li ZY: Study of anomalous I-V characteristics in spatially confined manganite structures. *Appl Phys Lett* 2007, **91**:102501.
- Singh-Bhalla G, Selcuk S, Dhakal T, Biswas A, Hebard AF: Intrinsic tunneling in phase separated manganites. *Phys Rev Lett* 2009, **102**:077205.
- Singh-Bhalla G, Biswas A, Hebard AF: Tunneling magnetoresistance in phase-separated manganite nanobridges. *Phys Rev B* 2009, **80**:144410.
- Shen J, Ward TZ, Yin LF: Emergent phenomena in manganites under spatial confinement. *Chin Phys B* 2013, **22**:017501.
- Wollan EO, Koehler WC: Neutron diffraction study of the magnetic properties of the series of perovskite-type compounds $[(1-x)\text{La}, x\text{Ca}]\text{MnO}_3$. *Phys Rev* 1955, **100**:545.
- Jonker GH, Van Santen JH: Ferromagnetic compounds of manganese with perovskite structure. *Physica* 1950, **16**:337.

38. Van Santen JH, Jonker GH: **Electrical conductivity of ferromagnetic compounds of manganese with perovskite structure.** *Physica* 1950, **16**:599.
39. Zener C: **Interaction between the d-shells in the transition metals.** *Phys Rev* 1951, **81**:440.
40. Searle CW, Wang ST: **Studies of the ionic ferromagnet (LaPb)MnO₃. V. Electric transport and ferromagnetic properties.** *Can J Phys* 1970, **48**:2023.
41. Jin S, Tiefel TH, McCormack M, Fastnacht RA, Ramesh R, Chen LH: **Thousandfold change in resistivity in magnetoresistive La-Ca-Mn-O films.** *Science* 1994, **264**:413.
42. Woodward PM, Cox DE, Vogt T, Rao CNR, Cheetham AK: **Effect of compositional fluctuations on the phase transitions in (Nd_{1/2}Sr_{1/2})MnO₃.** *Chem Mater* 1999, **11**:3528.
43. Fäth M, Freisem S, Menovsky AA, Tomioka Y, Aarts J, Mydosh JA: **Spatially inhomogeneous metal-insulator transition in doped manganites.** *Science* 1999, **285**:1540.
44. Mori S, Chen CH, Cheong SW: **Pairing of charge-ordered stripes in (La, Ca)MnO₃.** *Nature* 1998, **392**:473.
45. Renner C, Aeppli G, Kim BG, Soh YA, Cheong SW: **Atomic-scale images of charge ordering in a mixed-valence manganite.** *Nature* 2002, **416**:518.
46. De Teresa JM, Ibarra MR, Algarabel PA, Ritter C, Marquina C, Blasco J, Garcia J, del Moral A, Arnold Z: **Evidence for magnetic polarons in the magnetoresistive perovskites.** *Nature* 1997, **386**:256.
47. Zhang T, Zhou TF, Qian T, Li XG: **Particle size effects on interplay between charge ordering and magnetic properties in nanosized La_{0.25}Ca_{0.75}MnO₃.** *Phys Rev B* 2007, **76**:174415.
48. Zhu D, Zhu H, Zhang Y: **Hydrothermal synthesis of La_{0.5}Ba_{0.5}MnO₃ nanowires.** *Appl Phys Lett* 2002, **80**:1634.
49. Zhang T, Jin CG, Qian T, Lu XL, Bai JM, Li XG: **Hydrothermal synthesis of single-crystalline La_{0.5}Ca_{0.5}MnO₃ nanowires at low temperature.** *J Mater Chem* 2004, **14**:2787.
50. Li D, Wang Y, Xia Y: **Electrospinning of polymeric and ceramic nanofibers as uniaxially aligned arrays.** *Nano Lett* 2003, **3**:1167.
51. Jugdersuren B, Kang S, DiPietro RS, Heiman D, McKeown D, Pegg IL, Philip J: **Large low field magnetoresistance in La_{0.67}Sr_{0.33}MnO₃ nanowire devices.** *J Appl Phys* 2011, **109**:016109.
52. Shantha K, Raychaudhuri AK: **Growth of an ordered array of oriented manganite nanowires in alumina templates.** *Nanotechnol* 2004, **15**:1312.
53. Shankar KS, Kar S, Raychaudhuri AK, Subbanna GN: **Fabrication of ordered array of nanowires of La_{0.67}Ca_{0.33}MnO₃ (x = 0.33) in alumina templates with enhanced ferromagnetic transition temperature.** *Appl Phys Lett* 2004, **84**:993.
54. Curiale J, Sánchez RD, Troiani HE, Ramos CA, Pastoriza H, Leyva AG, Levy P: **Magnetism of manganite nanotubes constituted by assembled nanoparticles.** *Phys Rev B* 2007, **75**:224410.
55. Freeman MR, Choi BC: **Advances in magnetic microscopy.** *Science* 2001, **294**:1484.
56. Markovich V, Puzniak R, Mogilyansky D, Wu XD, Suzuki K, Fita I, Wisniewski A, Chen SJ, Gorodetsky G: **Exchange bias effect in La_{0.2}Ca_{0.8}MnO₃ antiferromagnetic nanoparticles with two ferromagnetic-like contributions.** *J Phys Chem C* 2011, **115**:1582.
57. Zhang T, Wang XP, Fang QF: **Evolution of the electronic phase separation with magnetic field in bulk and nanometer Pr_{0.67}Ca_{0.33}MnO₃ particles.** *J Phys Chem C* 2011, **115**:19482.
58. Kodama RH, Berkowitz AE, McNiff EJ Jr, Foner S: **Surface spin disorder in NiFe₂O₄ nanoparticles.** *Phys Rev Lett* 1996, **77**:394.
59. Wu JH, Lin JG: **Study on the phase separation of La_{0.75}Sr_{0.3}MnO₃ nanoparticles by electron magnetic resonance.** *J Magn Magn Mater* 2006, **304**:e7.
60. Yunoki S, Hu J, Malvezzi AL, Moreo A, Furukawa N, Dagotto E: **Phase separation in electronic models for manganites.** *Phys Rev Lett* 1998, **80**:845.
61. Han S, Li C, Liu ZQ, Lei B, Zhang DH, Jin W, Liu XL, Tang T, Zhou CW: **Transition metal oxide core-shell nanowires: generic synthesis and transport studies.** *Nano Lett* 2004, **4**:1241.
62. Nagashima K, Yanagida T, Tanaka H, Seki S, Saeki A, Tagawa S, Kawai T: **Effect of the heterointerface on transport properties of in situ formed MgO/titanate heterostructured nanowires.** *J Am Chem Soc* 2008, **130**:5378.
63. Li L, Li H, Zhai XF, Zeng CG: **Fabrication and magnetic properties of single-crystalline La_{0.33}Pr_{0.34}Ca_{0.33}MnO₃/MgO nanowires.** *Appl Phys Lett* 2013, **103**:113101.
64. Ghivelder L, Parisi F: **Dynamic phase separation in La_{5/8-y}Pr_yCa_{3/8}MnO₃.** *Phys Rev B* 2005, **71**:184425.
65. Niebieskikwiat D, Sanchez RD: **Pinning of elastic ferromagnetic/antiferromagnetic interfaces in phase-separated manganites.** *J Phys Condens Matter* 2012, **24**:436001.
66. Marín L, Morellón L, Algarabel PA, Rodríguez LA, Magén C, De Teresa JM, Ibarra MR: **Enhanced magnetotransport in nanopatterned manganite nanowires.** *Nano Lett* 2014, **14**:423.
67. Postma HWC, Teepen T, Yao Z, Grifoni M, Dekker C: **Carbon nanotube single-electron transistors at room temperature.** *Science* 2001, **293**:76.
68. Wolf SA, Awschalom DD, Buhrman RA, Daughton JM, Von Molnár S, Roukes ML, Chtchelkanova AY, Treger DM: **Spintronics: a spin-based electronics vision for the future.** *Science* 2001, **294**:1488–1495.
69. Tseng GY, Ellenbogen JC: **Toward nanocomputers.** *Science* 2001, **294**:1293.
70. Bachtold A, Hadley P, Nakanishi T, Dekker C: **Logic circuits with carbon nanotube transistors.** *Science* 2001, **294**:1317.
71. Hueso L, Mathur ND: **Nanotechnology: dreams of a hollow future.** *Nature* 2004, **427**:301.
72. Levy P, Leyva AG, Troiani H, Sánchez RD: **Nanotubes of rare-earth manganese oxide.** *Appl Phys Lett* 2003, **83**:5247.
73. Leyva AG, Stolar P, Rosenbusch M, Lorenzo V, Levy P, Albonetti C, Cavallini M, Biscarini F, Troiani HE, Curiale J, Sánchez RD: **Microwave assisted synthesis of manganese mixed oxide nanostructures using plastic templates.** *J Solid State Chem* 2004, **177**:3949.
74. Cullity BD: *Introduction to Magnetic Materials.* Reading, USA: Addison-Wesley; 1972.
75. Ward TZ, Gai Z, Xu XY, Guo HW, Yin LF, Shen J: **Tuning the metal-insulator transition in manganite films through surface exchange coupling with magnetic nanodots.** *Phys Rev Lett* 2011, **106**:157207.
76. Wu T, Mitchnell JF: **Creation and annihilation of conducting filaments in mesoscopic manganite structures.** *Phys Rev B* 2006, **74**:214423.
77. Guo X, Li PG, Wang X, Fu XL, Chen LM, Lei M, Zheng W, Tang WH: **Anomalous positive magnetoresistance effect in La_{0.67}Ca_{0.33}MnO₃ microbridges.** *J Alloy Compd* 2009, **485**:802.
78. Arnal T, Khvalkovskii AV, Bibes M, Mercey B, Lecoer P, Haghiri-Gosnet AM: **Electronic properties of domain walls in La_{2/3}Sr_{1/3}MnO₃: magnetotransport measurements on a nanopatterned device.** *Phys Rev B* 2007, **75**:220409.
79. Beekman C, Zaanen J, Aarts J: **Nonlinear mesoscopic transport in a strongly cooperative electron system: The La_{0.67}Ca_{0.33}MnO₃ microbridge.** *Phys Rev B* 2011, **83**:235128.
80. Beekman C, Komissarov I, Aarts J: **Large electric-field effects on the resistance of La_{0.67}Ca_{0.33}MnO₃ microstructures.** *Phys Rev B* 2012, **85**:245115.
81. Pallecchi I, Pellegrino L, Caviglia A, Bellingeri E, Canu G, Gazzadi GC, Siri AS, Marré D: **Current-driven hysteresis effects in manganite spintronics devices.** *Phys Rev B* 2006, **74**:014434.
82. Pallecchi I, Gadaleta A, Pellegrino L, Gazzadi GC, Bellingeri E, Siri AS, Marré D: **Probing of micromagnetic configuration in manganite channels by transport measurements.** *Phys Rev B* 2007, **76**:174401.
83. Ruotolo A, Orpallo A, Miletto Granozio F, Pepe GP, Perna P, Uccio USD, Pullini D: **Current-induced domain wall depinning and magnetoresistance in La_{0.75}Sr_{0.3}MnO₃ planar spin valves.** *Appl Phys Lett* 2007, **91**:132502.
84. Céspedes O, Watts SM, Coey JMD, Dörr K, Ziese M: **Magnetoresistance and electrical hysteresis in stable half-metallic La_{0.75}Sr_{0.3}MnO₃ and Fe₃O₄ nanostructures.** *Appl Phys Lett* 2005, **87**:083102.
85. Bhalla GS: *Size Effects in Phase Separated Manganite Nanostructures.* Florida, USA: Ph. D. Thesis. University of Florida; 2009.
86. Nakajima T, Tsuchiya T, Ueda Y, Kumagai T: **Probing electronic-phase-separated insulating domains in the metallic phase of patterned perovskite manganite microwires.** *Phys Rev B* 2009, **80**:020401.
87. Dagotto E, Yunoki S, Malvezzi AL, Moreo A, Hu J, Capponi S, Poilblanc D, Furukawa N: **Ferromagnetic Kondo model for manganites: phase diagram, charge segregation, and influence of quantum localized spins.** *Phys Rev B* 1998, **58**:6414.
88. Dagotto E: *Nanoscale Phase Separation and Colossal Magnetoresistance.* Berlin, Germany: Springer; 2003.
89. Yunoki S, Moreo A, Dagotto E: **Phase separation induced by orbital degrees of freedom in models for manganites with Jahn-Teller phonons.** *Phys Rev Lett* 1998, **81**:5612.
90. Moreo A, Yunoki S, Dagotto E: **Phase separation scenario for manganese oxides and related materials.** *Science* 1999, **283**:2034.

91. Ahn KH, Lookman T, Bishop AR: **Strain-induced metal–insulator phase coexistence in perovskite manganites.** *Nature* 2004, **428**:401.
92. Ramakrishnan TV, Krishnamurthy HR, Hassan SR, Pai GV: **Theory of insulator metal transition and colossal magnetoresistance in doped manganites.** *Phys Rev Lett* 2004, **92**:157203.
93. Milward GC, Calderon MJ, Littlewood PB: **Electronically soft phases in manganites.** *Nature* 2005, **433**:607.

doi:10.1186/1556-276X-9-325

Cite this article as: Liang *et al.*: Research progress on electronic phase separation in low-dimensional perovskite manganite nanostructures. *Nanoscale Research Letters* 2014 **9**:325.

Submit your manuscript to a SpringerOpen[®] journal and benefit from:

- ▶ Convenient online submission
- ▶ Rigorous peer review
- ▶ Immediate publication on acceptance
- ▶ Open access: articles freely available online
- ▶ High visibility within the field
- ▶ Retaining the copyright to your article

Submit your next manuscript at ▶ springeropen.com
